Dynamics of skyrmions and vortices in antiferromagnets

Joren Harms*
Institute for Theoretical physics, Utrecht University
(Supervisor: Prof. dr. R.A. Duine)
(Dated: October 22, 2017)

ABSTRACT

Skyrmions are magnetic textures, that behave like particles. They exist as excitations within two-dimensional magnetic insulators and are promising candidates for future data storage. There has been a strong rise in interest in skyrmions in recent years, which is encouraged by several experimental observations of skyrmions in various magnetic thin-films. In this paper the classical dynamics of skyrmions and vortices in antiferromagnets are studied. We find that an antiferromagnetic skyrmion does not feel a Magnus force, while a ferromagnetic skyrmion does. We also see that an antiferromagnetic vortex feels a Magnus force.

KEYWORDS

Skyrmion, vortex, antiferromagnet.

I. INTRODUCTION

In a magnet textures can appear that behave like particles. These magnetic textures are phenomena that move in a collective way through a magnet and may thus be described as a single object.

The focus of this paper is on the classical dynamics of such a particle-like magnetic texture, namely skyrmions (see Fig. 1) [1]. There has been a strong rise in interest for skyrmions in recent years, which is stimulated by several experimental observations of skyrmions in various thin-film magnets [2–5]. Magnetic skyrmions are promising candidates for storing information, due to the fact that they are topologically stable in the sense that no continuous local deformation can destroy a skyrmion and they can be moved using relatively low currents.

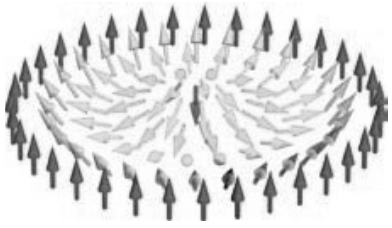

FIG. 1. Graphical depiction of a ferromagnetic skyrmion. *Nature nanotechnology 8.3 (2013): 152-156.*

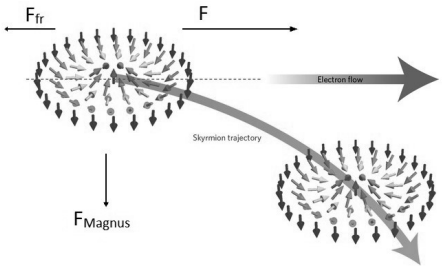

FIG. 2. Magnus force for ferromagnetic skyrmion with winding number one. *Nature Physics 13.2 (2017): 112-113.*

The main findings of this paper are:

1. An antiferromagnetic skyrmion does not experience a Magnus force, which is in agreement with Ref. [6]. This is different from a ferromagnetic skyrmion, which does feel a Magnus force. It will also have a classical mass opposite to a ferromagnetic skyrmion, which is massless if interactions with e.g. spin waves are neglected. *The Magnus force will give rise to motion perpendicular to the direction of the applied force (see Fig. 2). This type of force also appears in e.g. a rotating ball or a vortex in a fluid.*

2. For magnetic fields above the spin flop field we find vortex configurations (see Section III B) which feel a Magnus force which is proportional to the magnetic field.

The remainder of this paper is organized as follows. In Section II the dynamics of antiferromagnets is described and an action which only depends on the Néel vector is derived. This is done by integrating out the magnetic field, assuming both large wavelengths for both the Néel vector and the magnetization. In Section III the profile of a single antiferromagnetic skyrmion is determined and another topologically protected structure is introduced, which is called a vortex. In Section IV the classical dynamics (no spin wave interactions) of skyrmions and vortices in two-dimensional antiferromagnets are determined.

* j.s.harms@students.uu.nl;

II. DYNAMICS OF ANTIFERROMAGNETS

In a ferromagnet the exchange interaction wants to align two neighboring spins. In an antiferromagnet, the exchange interaction forces neighboring spins to point in opposite directions (see Fig. 3).

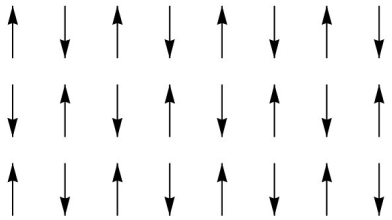

FIG. 3. A graphical example of antiferromagnetic ordering.

The aim of this section is to describe antiferromagnetic motion in the imaginary time path integral formalism. It turns out that Haldane's mapping is useful for describing antiferromagnet dynamics. In Section II A we work out the kinetic term/Berry phase for our system, using Haldane's mapping. We expect the magnetic moments due to an external magnetic field to be small due to a large antiferromagnetic exchange interaction. This allows us to make an expansion of the Hamiltonian up to second order in the canting field (magnetic moments) $\mathbf{m}$. Most methods used in this section are described in Ref. [7].

Haldane's mapping is useful to make a distinction between short and long wavelength fluctuations. In this paper we will be looking at long wavelength fluctuations around a single skyrmion configuration. We start by introducing two continuous vector fields $(\mathbf{n}, \mathbf{m})$, such that:

$$\mathbf{\Omega}_i = \eta_i \hat{\mathbf{n}}(\mathbf{x}_i)\sqrt{1-|\mathbf{m}(\mathbf{x}_i)|^2} + \mathbf{m}(\mathbf{x}_i) \tag{1}$$

with $\eta_i = e^{i\mathbf{x}_i\cdot\vec{\pi}}$, $\hat{\mathbf{n}}$ is called the Néel vector and $\mathbf{m}$ the canting field. Furthermore $|\hat{\mathbf{n}}(\mathbf{x}_i)| = 1$ and $\hat{\mathbf{n}}(\mathbf{x}_i)\cdot\mathbf{m}(\mathbf{x}_i) = 0$.

A. The Kinetic term / Berry phase

From Ref. [8, Appendix A] it follows that the Berry phase of the total system is given by the sum over all the independent Berry phases, which is given by

$$\mathcal{A}_B[\{\mathbf{\Omega}\}] = iS\sum_i \omega[\mathbf{\Omega}_i] = iS\sum_i \int_0^\beta \mathbf{A}[\mathbf{\Omega}_i]\partial_\tau \mathbf{\Omega}_i. \tag{2}$$

Here the sum over i means a sum over all the lattice points and A is a gauge invariant vector field with the property that $\nabla_\Omega \cdot A_i = \mathbf{\Omega}_i$.

Considering only large wavelengths and expanding Eq. (2) up to second order in $\mathbf{m}$, we obtain

$$\mathcal{A}_B[\{\mathbf{\Omega}\}] \approx i\frac{S}{a^2}\int \mathrm{d}\tau \int \mathrm{d}\mathbf{x}\,\{\hat{\mathbf{n}}(\mathbf{x})\times\partial_\tau\hat{\mathbf{n}}(\mathbf{x})\cdot\mathbf{m}(\mathbf{x})\}. \tag{3}$$

B. The partition function

In this section we start from the following Hamiltonian:

$$\mathcal{H} = \frac{1}{2}\sum_{\langle ij\rangle}\Big\{S^2 J_{ij}\hat{\mathbf{\Omega}}_i\cdot\hat{\mathbf{\Omega}}_j + S^2\mathbf{D}_{ij}\left(\hat{\mathbf{\Omega}}_i\times\hat{\mathbf{\Omega}}_j\right) - S^2\tilde{K}_z^a\hat{\mathbf{\Omega}}_{z,i}^2 - S\mathbf{H}\cdot\mathbf{\Omega}_i\Big\}. \tag{4}$$

$J_{ij} > 0$ is the Heisenberg exchange interaction (which is positive in the antiferromagnetic case), D_{ij} gives the Dzyaloshinskii-Moriya exchange interaction, K_z gives the anisotropy of the system and $\mathbf{H}$ represents an external magnetic field. We assume that both J_{ij} and D_{ij} have the full lattice symmetry.

The action describing antiferromagnetic dynamics is given by the Berry phase plus the Hamiltonian. By expanding both up to second order in $\mathbf{m}$ and integrating out this canting field we obtain the following action which only depends on the Néel vector

$$\mathcal{S}_E[\hat{\mathbf{n}}] \approx N_A\int_0^\beta \mathrm{d}\tau\int_\Lambda \mathrm{d}\mathbf{x}\Big\{\frac{1}{2}\chi_0|\partial_\tau\hat{\mathbf{n}}(\mathbf{x})|^2 + i\chi_0\tilde{H}(\hat{\mathbf{n}}(\mathbf{x})\times\partial_\tau\hat{\mathbf{n}}(\mathbf{x}))^z\Big\} + \mathcal{F}[\hat{\mathbf{n}}], \tag{5}$$

$$\mathcal{F}[\hat{\mathbf{n}}] = N_A\int_\Lambda \mathrm{d}\mathbf{x}\Big\{\frac{\rho_s}{2}\sum_{l=x,y}|\partial_l\hat{\mathbf{n}}|^2 + \frac{D}{2}\left(\hat{y}\cdot\left(\hat{\mathbf{n}}\times\frac{\partial\hat{\mathbf{n}}}{\partial x}\right) - \hat{x}\cdot\left(\hat{\mathbf{n}}\times\frac{\partial\hat{\mathbf{n}}}{\partial y}\right)\right) - K_z\hat{\mathbf{n}}_z^2 + \frac{\chi_0}{2}\left(\tilde{\mathbf{H}}\cdot\hat{\mathbf{n}}(\mathbf{x})\right)^2\Big\}. \tag{6}$$

Where N_A is given by the number of antiferromagnetic layers along the $\hat{z}$-direction and χ_0 is the uniform susceptibility. We also assume that the magnetic field is pointing in the $\hat{z}$-direction.

III. PROFILE OF ANTIFERROMAGNETIC SKYRMION

A. Minimizing the free energy of the antiferromagnet

In this section we determine the Euler-Lagrange equations belonging to the energy in Eq. (6). Now we use the transformation

$$\hat{\mathbf{n}} = \sin[\theta]\cos[\phi_0]\,\hat{\rho} + \sin[\theta]\sin[\phi_0]\,\hat{\phi} + \cos[\theta]\,\hat{z}.$$

The given Hamiltonian is translationally invariant and the skyrmion configuration is a local minimum of the Hamiltonian in Eq. (6). Because of this the skyrmion configuration will be rotationally invariant. We assume

θ only depends on ρ and ϕ_0 is constant. We also choose the magnetic field to be in the $\hat{z}$-direction. Using the preceding assumptions the Hamiltonian in Eq. (6) reduces to

$$\begin{aligned}\mathcal{F}[\hat{\mathbf{n}}] = 2\pi N_A \int_\Lambda \Bigg\{ & \frac{\rho_s}{2}\left((\partial_\rho\theta)^2 + \frac{\sin^2(\theta)}{\rho^2}\right) \\ & + \frac{D}{2}\cos(\phi_0)\left(\partial_\rho\theta + \frac{\cos(\theta)\sin(\theta)}{\rho}\right) \\ & - K_z\cos^2(\theta) + \frac{\chi_0}{2}\tilde{H}^2\cos^2(\theta)\Bigg\}\rho d\rho.\end{aligned} \tag{7}$$

The skyrmion configuration will be a local minimum in the energy (i.e. $\frac{\delta\mathcal{F}}{\delta\theta} = 0$) with boundary conditions $\theta(0) = \pi$ and $\theta(\infty) = 0$. By performing the substitution $\tilde{\rho} = \sqrt{\frac{K_z}{\rho_s}}\rho$ in Eq. (7) and multiplying the total by $\frac{\rho_s}{K_z}$, we obtain the following dimensionless Euler-Lagrange equation

$$\begin{aligned}&\left(\frac{\partial^2\theta}{\partial\tilde{\rho}^2} + \frac{1}{\tilde{\rho}}\frac{\partial\theta}{\partial\tilde{\rho}} - \frac{\sin(\theta)\cos(\theta)}{\tilde{\rho}^2}\right) \\ &+ \frac{4D}{\pi D_0}\cos(\phi_0)\frac{\sin^2(\theta)}{\tilde{\rho}} - \left(1 - \frac{h^2}{h_0^2}\right)\sin(2\theta) = 0.\end{aligned} \tag{8}$$

In the preceding equation we used $D_0 = (4/\pi)\sqrt{\rho_s K_z}$, $h^2 = \frac{\chi_0}{2}\tilde{H}^2$ and $h_0 = \sqrt{K_z}$.

B. Finding local skyrmion solutions

First note that there are different type of solutions for different values of $\frac{h}{h_0}$. To see this, one must notice that h_0 is the spin flop field. When $h = h_0$ the Néel vector flops into the basal plane and for $h > h_0$ the magnetic field gives rise to a magnetization (see Fig. 4). This causes weak ferromagnet behavior. When $h < h_0$ we get solutions with boundary conditions $\theta(0) = \pi$ and $\theta(\infty) = 0$. At the moment $h > h_0$ we also get solutions with boundary conditions $\theta(0) = \pi$ and $\theta(\infty) = \pi/2$.

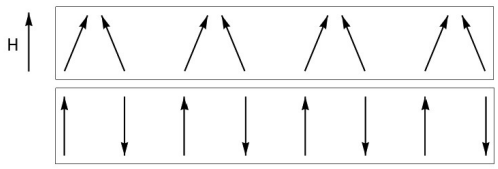

FIG. 4. Graphical depiction of an antiferromagnetic state when the magnetic field is above the spin flop field ($h > h_0$) and antiferromagnetic ordering when the magnetic field is far below the spin flop field ($h < h_0$).

C. Small magnetic field $h/h_0 = 0.3$

Now we consider the case in which $h/h_0 = 0.3$. We see that the radii of the skyrmions grow as $d = D/D_0$ increases (see Fig. 5). We conclude that antiferromagnetic skyrmions have a size of order $\mathcal{O}(\sqrt{\rho_s/K_z})$.

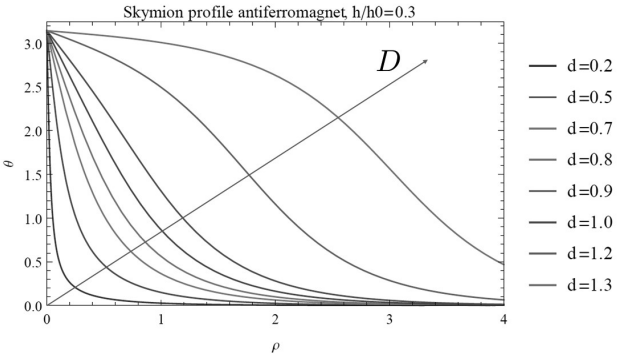

FIG. 5. Skyrmion configuration for $D/D_0 \in \{0.2, 0.5, 0.7, 0.8, 0.9, 1.0, 1.2, 1.30\}$ with $h/h_0 = 0.3$.

IV. CLASSICAL DYNAMICS OF ANTIFERROMAGNETIC SKYRMIONS

In Section II we found that the action describing antiferromagnetic dynamics is given by

$$\begin{aligned}\mathcal{S}_E[\hat{\mathbf{n}}] \approx N_A \int_0^\beta d\tau \int_\Lambda d\mathbf{x}\Bigg\{ & \frac{1}{2}\chi_0|\partial_\tau\hat{\mathbf{n}}(\mathbf{x})|^2 \\ & + i\chi_0\tilde{H}(\hat{\mathbf{n}}(\mathbf{x})\times\partial_\tau\hat{\mathbf{n}}(\mathbf{x}))^z\Bigg\} + \mathcal{F}[\hat{\mathbf{n}}].\end{aligned} \tag{9}$$

A. Dynamics of non-interacting antiferromagnetic skyrmion

Since $\hat{\mathbf{n}}$ is always a unit vector it will be useful to describe it using polar coordinates

$$\begin{aligned}&\hat{\mathbf{n}}(\mathbf{x},\tau) = \\ &\{\sin[\theta_0(\mathbf{x},\tau)]\cos[\phi_0], \sin[\theta_0(\mathbf{x},\tau)]\sin[\phi_0], \cos[\theta_0(\mathbf{x},\tau)]\}\end{aligned} \tag{10}$$

The skyrmion configuration will characterized by the collective dynamical coordinate $\mathbf{R}(\tau)$

$$\theta_0(\mathbf{x} - \mathbf{R}(\tau)), \tag{11}$$

$$\phi_0(\mathbf{x} - \mathbf{R}(\tau)). \tag{12}$$

In Eqs. (13) and (14) we calculate the classical part of the dynamical terms in Eq. (9), Eq. (13) reduces to a

mass and Eq. (14) gives rise to a Magnus force,

$$\begin{aligned}
&\int \mathrm{d}\tau\mathrm{d}\mathbf{x}|\partial_\tau \hat{\mathbf{n}}_\mathbf{0}|^2 = \int \mathrm{d}\tau\mathrm{d}\mathbf{x}\left|\partial_\beta \hat{\mathbf{n}}_\mathbf{0}\dot{R}^\beta\right|^2 \\
&= \int \mathrm{d}\tau \tilde{M}_{\beta\gamma}\dot{R}^\alpha\dot{R}^\gamma, \\
&\int \mathrm{d}\tau\mathrm{d}\mathbf{x}\ (\hat{\mathbf{n}}_\mathbf{0}\times\partial_\tau\hat{\mathbf{n}}_\mathbf{0})^z \\
&\rightarrow \int \mathrm{d}\tau \dot{R}^i R^j \left\{\int \mathrm{d}\mathbf{x}\ 2(\partial_i\hat{\mathbf{n}}_\mathbf{0}\times\partial_j\hat{\mathbf{n}}_\mathbf{0})^z\right\} \\
&= \int d\tau \left\{\tilde{\alpha}\epsilon_{ij}R^i\dot{R}^j\right\}.
\end{aligned} \tag{13}$$

(14)

In Eq. (14) we used that the skyrmion configuration is rotationally invariant. Using this rotational invariance it follows that the mass matrix $\tilde{M}$ is diagonal. We define $M = \chi_0\tilde{M}$ and $\alpha = \chi_0\tilde{H}\tilde{\alpha}$. By writing $\mathbf{x}$ in cylindrical coordinates $(x = \rho\cos(\theta)), y = \rho\sin(\theta))$ and performing the transformation $\tilde{\rho} = \sqrt{(K_z/\rho_s)}\ \rho$ on $\tilde{M}$ and $\tilde{\alpha}$ we obtain

$$\begin{aligned}
M = 2\pi\chi_0 \int_0^\infty d\tilde{\rho} \Big\{ &\tilde{\rho}\left(\partial_{\tilde{\rho}}\hat{\mathbf{n}}_\mathbf{0}\right)^2 \\
&+ \frac{1}{\tilde{\rho}}\left\{\sin(\theta_0)\sin(\phi_0)\hat{\rho} - \sin(\theta_0)\cos(\phi_0)\hat{\phi}\right\}^2\Big\},
\end{aligned} \tag{15}$$

$$\alpha = 2\pi\tilde{H}\chi_0\sin^2(\theta(\rho))\big|_{\rho=0}^{\rho=\infty}. \tag{16}$$

Since the dimensionless integral in Eq. (15) takes on values between zero and ten for different skyrmion configurations we obtained in Section III, we see that M roughly has order of magnitude $\mathcal{O}(\chi_0)$ if D/D_0 is of order one. For skymions with winding number $n \in \mathbb{Z}$, α in Eq. (16) will be zero. So antiferromagnetic skyrmions do not feel a Magnus force, which is in agreement with Ref. [6]. For magnetic fields above the spin-flop field, vortices may arise. Vortices have different boundary conditions than skyrmions for which α is non-zero, which implies that antiferromagnetic vortices feel a Magnus force. For the boundary conditions of the vortex ($\theta_0(0) = \pi$ and $\theta_0(\infty) = \pi/2$), we see that $\alpha = -2\pi\tilde{H}\chi_0$.

The classical action (no interactions) describing the dynamics of skyrmions or vortices is thus given by

$$\mathcal{S}_{cl} = N_A\int_0^\beta \mathrm{d}\tau\left\{\frac{1}{2}M\dot{R}^2 + i\alpha\epsilon_{ij}R^i\dot{R}^j\right\}. \tag{17}$$

V. CONCLUSIONS

In this paper we gave a description for the classical dynamics of skyrmions in antiferromagnetic thin-films. In Section II long wavelengths for $\hat{\mathbf{n}}$ and $\mathbf{m}$ were assumed. By integrating out the magnetization in the action that describes the antiferromagnetic dynamics we were able to derive the action given in Eq. (5) which is only dependent on the Néel field $\hat{\mathbf{n}}$. We derived that antiferromagnetic skyrmions have a classical mass and feel no Magnus force, which is in agreement with Ref. [6]. This result differs from ferromagnetic skyrmions, which feel a Magnus force and have no classical mass [9]. We also find that a vortex does feel a Magnus force, since the boundary conditions of a vortex are different from those of a skyrmion.

VI. ROLE OF THE STUDENT

Joren Harms is an undergraduate student working under the supervision of Rembert Duine. The topic was chosen by Rembert Duine and the research was done by Joren Harms. This includes the problem definition, obtaining the results and conclusions for the project. During the past year Joren regularly met with his supervisor to discuss the results and possible future directions. This paper reflects just a part of the thesis [10].

ACKNOWLEDGEMENTS

First and most foremost I would like to thank my supervisor R.A. Duine, for his guidance through this project. Secondly I would like to thank C. Psaroudaki for a helpful discussion.

[1] T. Skyrme, Nuclear Physics **31**, 556 (1962).

[2] S. Mühlbauer, B. Binz, F. Jonietz, C. Pfleiderer, A. Rosch, A. Neubauer, R. Georgii, and P. Böni, Science **323**, 915 (2009), http://science.sciencemag.org/content/323/5916/915.full.pdf.

[3] S. Heinze, K. Von Bergmann, M. Menzel, J. Brede, A. Kubetzka, R. Wiesendanger, G. Bihlmayer, and S. Blügel, Nature Physics **7**, 713 (2011).

[4] I. Raičević, D. Popović, C. Panagopoulos, L. Benfatto, M. B. Silva Neto, E. S. Choi, and T. Sasagawa, Phys. Rev. Lett. **106**, 227206 (2011).

[5] A. Neubauer, C. Pfleiderer, B. Binz, A. Rosch, R. Ritz, P. G. Niklowitz, and P. Böni, Phys. Rev. Lett. **102**, 186602 (2009).

[6] J. Barker and O. A. Tretiakov, Phys. Rev. Lett. **116**, 147203 (2016).

[7] A. Auerbach, *Interacting Electrons and Quantum Magnetism* (Springer-Verlag New York).

[8] H.-B. Braun and D. Loss, Phys. Rev. B **53**, 3237 (1996).

[9] C. Psaroudaki, S. Hoffman, J. Klinovaja, and D. Loss, ArXiv e-prints (2016), arXiv:1612.01885 [cond-mat.mes-hall].

[10] J. Harms, "Quantum dynamics of skyrmions and vortices in antiferromagnets," (2017), Utrecht University.